

CERN-TH/97-193

ITP-SB-97-48

hep-ph/9708261

# Model-independent QED corrections to photon structure-function measurements<sup>a</sup>

Eric Laenen

*Institute for Theoretical Physics, State University of New York at Stony Brook,  
Stony Brook, NY 11794, USA*

E-mail: [eric@insti.physics.sunysb.edu](mailto:eric@insti.physics.sunysb.edu)

and

Gerhard A. Schuler<sup>b</sup>

*Theory Division, CERN,  
CH-1211 Geneva 23, Switzerland*

E-mail: [Gerhard.Schuler@cern.ch](mailto:Gerhard.Schuler@cern.ch)

## Abstract

We present the first calculation of QED radiative corrections to deep-inelastic electron–photon scattering in terms of those variables that are reconstructed in measurements of the photon structure function in electron–positron collisions. In order to cover the low- $Q^2$  region, we do not invoke the QCD-improved parton model but rather express our results in terms of the photon structure functions. Both analytical and numerical results are given.

---

<sup>a</sup> Talk presented at the XIth Workshop on Photon–Photon Collisions, Photon '97, Egmond aan Zee, The Netherlands.

<sup>b</sup> Heisenberg Fellow.

QED radiative corrections distort the usual kinematics of deep-inelastic scattering (DIS) and hence have to be taken into account for precise structure-function measurements. In the case of the proton structure function, the Born kinematics (corresponding to non-radiative events) of charged lepton–nucleon scattering is fully constrained by two measurable variables. The arguments of  $F_2(x, Q^2)$ , Bjorken- $x$  and the squared momentum transfer  $Q^2$ , can directly be determined from either the scattered lepton or the hadronic system. Alternatively, the kinematics can be fixed by two “mixed” variables such as the polar angles of the scattered lepton and the hadronic system. Photon radiation affects different variables differently but, in general, several variables can be reconstructed experimentally and hence one can have experimental cross checks on the size of radiative corrections [1].

The situation is more complicated for measurements of the photon structure function in electron–positron collisions. At given  $e^+e^-$  c.m. energy  $\sqrt{s} = 2E_b$  ( $E_b$  is the beam energy), three variables are needed in order to specify the Born kinematics since the target-photon energy is not known. (Actually, for precision measurements also the effects of the non-zero target mass  $P^2$  have to be considered.) Moreover, there is just one way to experimentally reconstruct three independent variables.

The angle  $\theta$  and energy  $E$  of the tagged electron give the leptonic DIS variables  $y_l$  and  $Q_l^2$  as follows:

$$y_l = 1 - \frac{E}{E_b} \cos^2 \frac{\theta}{2}, \quad Q_l^2 = 4 E E_b \sin^2 \frac{\theta}{2}. \quad (1)$$

A measurement of the hadronic mass  $W_h$  (which involves an unfolding of  $W_h$  from the visible hadronic energy  $W_{\text{vis}}$ ) yields the “mixed” Bjorken- $x$  variable

$$x_m = \frac{Q_l^2}{Q_l^2 + W_h^2}. \quad (2)$$

In general, neither  $x_m$  nor  $Q_l$  coincide with the actual arguments  $x_h$  and  $Q_h$  of the photon structure function  $F_2(x_h, Q_h^2)$ , see e.g. (13) or Fig. 3 below. Consider DIS of electrons on (quasi-real) photons in the presence of an additional photon (Fig. 1):

$$e(l) + \gamma(p) \rightarrow e(l') + \gamma(k) + X(p_X), \quad (3)$$

and define leptonic and hadronic DIS variables:

$$\begin{aligned} q_l &= l - l' & q_h &= p_X - p = q_l - k \\ W_l^2 &= (p + q_l)^2 & W_h^2 &= (p + q_h)^2 = p_X^2 \\ Q_l^2 &= -q_l^2 & Q_h^2 &= -q_h^2 \\ x_l &= Q_l^2/2p \cdot q_l & x_h &= Q_h^2/2p \cdot q_h \\ y_l &= p \cdot q_l/p \cdot l & y_h &= p \cdot q_h/p \cdot l \end{aligned} \quad (4)$$

Obviously, leptonic and hadronic variables do not coincide ( $Q_h^2 \neq Q_l^2$ , etc.); they agree only for nonradiative events, i.e. if  $k = 0$ .

In this paper we present the  $O(\alpha)$  correction to DIS in terms of the experimentally relevant variables  $x_m$ ,  $Q_l^2$ , and  $y_l$ :

$$\frac{d^3\sigma}{dx_m dy_l dQ_l^2} = g^{\text{B}}(x_m, y_l, Q_l^2, s) + g^{\text{corr}}(x_m, y_l, Q_l^2, s). \quad (5)$$

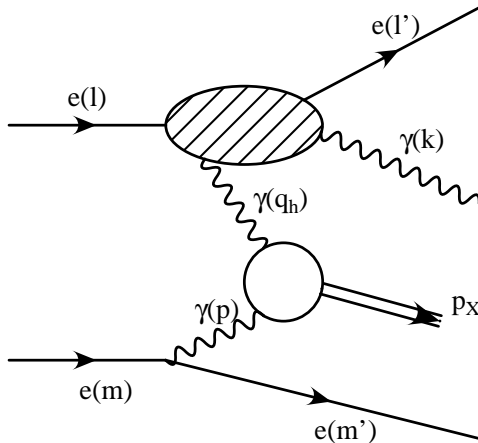


Figure 1: Photon bremsstrahlung from the tagged lepton line in deep-inelastic scattering off an equivalent photon.

Since the accessible  $Q$  values are far below the weak scale, we can safely neglect weak corrections apart from the running of the electromagnetic coupling  $\alpha(Q^2)$ . For the case of charged lepton–nucleon scattering it is known [2] that QED corrections are very well approximated by calculations in the leading-log approximation (LLA), that is the QED corrections are dominated by photon radiation off the tagged-lepton line (Fig. 1). For the case of electron–photon scattering, there might be additional, sizeable corrections to the untagged electron line. However, we shall show in the next paragraph that these are, in fact, small.

The target photon  $\gamma(p)$  is part of the flux of equivalent photons around the non-tagged lepton. To leading order in  $\alpha$ , this flux has a momentum density given by the Weizsäcker-Williams expression  $f_{\gamma/e}(z)$ , where  $z$  is the longitudinal momentum fraction of the target photon with respect to its parent lepton:

$$f_{\gamma/e}(z) = \frac{\alpha}{2\pi} \left\{ \frac{Y_+(z)}{z} \ln \frac{P_{max}^2}{P_{min}^2} - 2m_e^2 z \left( \frac{1}{P_{min}^2} - \frac{1}{P_{max}^2} \right) \right\}. \quad (6)$$

Here we have defined  $Y_+(z) = 1 + (1-z)^2$ ,  $P_{min}^2 = (z^2 m_e^2)/(1-z)$ ,  $P_{max}^2 = (1-z)(E_b \theta_{max})^2$ , and  $\theta_{max}$  is the anti-tag<sup>1</sup> angle. In the following we put  $P^2 \equiv -p^2 = 0$  and neglect electron masses everywhere except in (6). Moreover we substitute  $P_{max}^2$  by  $P_{max}^2 + P_{min}^2$  so that we can easily extend the  $z$  range to 1. QED radiative corrections to this formula follow immediately from our previous paper [3]. The corrections can (and must) be resummed and, within the LLA, the corrected expression is obtained by replacing  $Y_+(z)$  in (6) by  $Z_+(z, \mu^2)$  defined by

$$Z_+(z, \mu^2) = Y_+(z) \left\{ \exp \left[ \frac{\alpha}{\pi} \left( \ln \frac{Q^2}{m_e^2} - 1 \right) \ln(1-z) \right] \right\} + \frac{\alpha}{\pi} \ln \frac{Q^2}{m_e^2} \left\{ z \left( 1 - \frac{z}{2} \right) \ln z + z \left( 1 - \frac{z}{4} \right) \right\} \quad (7)$$

Here  $\mu$  is the hard scale of the photon-induced subprocess. A numerical evaluation of (7) shows that the corrections are indeed small, below the few-percent level.

<sup>1</sup>i.e. all events in which the parent lepton scatters at an angle larger than  $\theta_{max}$  are rejected.

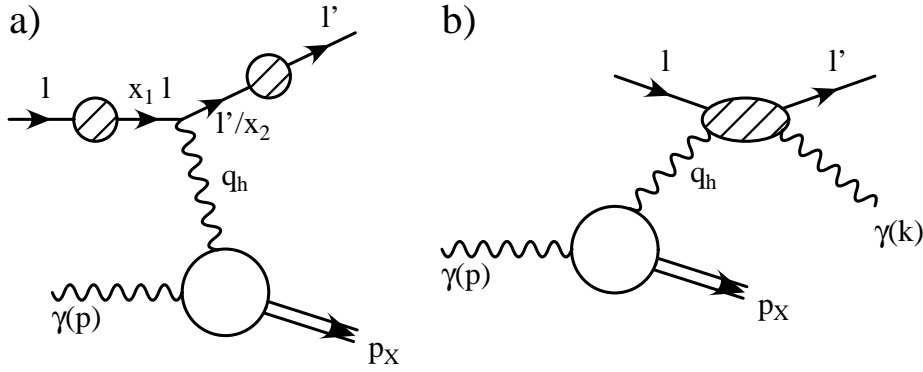


Figure 2: a) Initial- and final state bremsstrahlung. b) Compton contribution.

The Born cross section of (5) is given by

$$g^B(x, y, Q^2, s) = \frac{2\pi\alpha^2 Y_+(y)}{x^2 y^2 s Q^2} f_{\gamma/e}\left(\frac{Q^2}{xy s}\right) F_2(x, Q^2) \{1 + R(x, Q^2, y)\}, \quad (8)$$

where

$$R(x, Q^2, y) = \frac{-y^2}{1 + (1 - y)^2} \frac{F_L(x, Q^2)}{F_2(x, Q^2)}, \quad (9)$$

and  $F_{2,L}$  are the photon structure functions (we have dropped the superscript  $\gamma$ ).

In the LLA, photon radiation from the tagged lepton line can (in a gauge-invariant way) be subdivided into photon bremsstrahlung from the initial electron line, the final electron line, and the Compton process, see Fig. 2. For the cross section relevant for experimental analyses, which is differential in  $x_m$ ,  $Q_l^2$ , and  $y_l$ , there is no contribution from final-state radiation as the calorimeter measurement combines the electron with the nearby photon(s).

The initial state radiation correction to the triple differential cross section in eq. (5) can be written as the following convolution

$$g^{\text{ISR}}(x_m, y_l, Q_l^2, s) = \int_0^1 dx_1 D_{e/e}(x_1, Q_l^2) \left[ \Theta(x_1 - x_1^0) \frac{\hat{x}_m^2}{x_m^2 x_1} g^B(\hat{x}_m, \hat{y}_l, \hat{Q}_l^2, \hat{s}) - g^B(x_m, y_l, Q_l^2, s) \right] \quad (10)$$

where

$$x_1^0 \equiv \frac{x_m(1 - y_l)s + (1 - x_m)Q_l^2}{x_m(s - Q_l^2)}, \quad (11)$$

and  $D_{e/e}(x, Q^2)$  is the structure function for the initial-state electron evaluated at the scale given by the squared momentum transfer  $Q^2 = Q_l^2$ :

$$D_{e/e}(x, Q^2) = \frac{\alpha}{2\pi} \ln\left(\frac{Q^2}{m_e^2}\right) \frac{1 + x^2}{1 - x}. \quad (12)$$

It represents the probability of finding, inside a parent electron, an electron with longitudinal momentum fraction  $x$ . The Born cross section is written in terms of the reduced

Table 1: Corrections in per cents due to initial-state radiation (parameters see text).

$Q_l^2/\text{GeV}^2$								
$10^4 c$								3.3
$10^4$							-11.6	-2.1
$10^3 c$						-14.6	-7.3	-1.9
$10^3$					-15.6	-8.4	-4.8	-1.1
$10^2 c$				-15.9	-8.6	-5.3	-3.4	-0.6
$10^2$			-16.0	-8.7	-5.3	-3.8	-2.6	-0.3
$10^1 c$		-16.1	-8.9	-5.4	-3.6	-2.9	-2.0	-0.4
10	-17.3	-8.5	-3.7	-0.3	2.0	3.6	5.2	6.5
$c/10^{-4}$	$c 10^{-4}$	$10^{-3}$	$c 10^{-3}$	$10^{-2}$	$c 10^{-2}$	$10^{-1}$	$c 10^{-1}$	1
$x_m \quad (c = \sqrt{10} \approx 3.16)$								

(“hatted”) variables,  $g^{\text{B}}(\hat{x}_m, \hat{y}_l, \hat{Q}_l^2, \hat{s})$ . The scaling behavior of the relevant variables is

$$\begin{aligned} \hat{Q}_l^2 &= x_1 Q_l^2 = Q_h^2, & \hat{y}_l &= 1 - (1 - y_l)/x_1 = \frac{y_h}{x_1}, & \hat{s} &= x_1 s, \\ \hat{x}_m &= x_h = \frac{\hat{Q}_l^2}{\hat{Q}_l^2 + W_h^2} = \frac{x_m x_1}{x_1 + (1 - x_1)(1 - x_m)}. \end{aligned} \quad (13)$$

We find the following result for the Compton contribution to the total cross section

$$\sigma[ee \rightarrow eeX] = \frac{y_l dy_l}{1 - y_l} \frac{dx_m}{x_m (1 - x_m)} \frac{dQ_l^2}{Q_l^4} \frac{dz}{z} \frac{dQ_h^2}{Q_h^2} \frac{(1 - x_m) Q_l^2}{(1 - x_m) Q_l^2 + x_m Q_h^2} \Sigma, \quad (14)$$

where

$$\begin{aligned} \Sigma(x_h, x_l, y_l, Q_h^2, Q_l^2, z) &= \alpha^3 Y_+(y_l) z f_{\gamma/e}(z) \\ &\left\{ \left[ 1 + \left( 1 - \frac{x_l}{x_h} \right)^2 \right] F_2(x_h, Q_h^2) - \left( \frac{x_l}{x_h} \right)^2 F_L(x_h, Q_h^2) \right\}. \end{aligned} \quad (15)$$

Note that  $\Sigma$  is a very smooth function, hardly dependent on its arguments. Only at very low  $Q_h^2$ , gauge invariance forces  $F_2$  (and hence  $\Sigma$ ) to vanish linearly with  $Q_h^2 \rightarrow 0$ . The fall-off at  $x_h \rightarrow 1$  may be very slow due to the pointlike contribution to  $F_2^\gamma$  (in contrast to  $F_2^p$ ).

The argument  $x_h$  of  $F_2$  is here related to the integration variables via

$$x_h = \frac{x_m Q_h^2}{(1 - x_m) Q_l^2 + x_m Q_h^2}, \quad (16)$$

Table 2: Corrections in per **mille** due to the Compton process (parameters see text).

$Q_l^2/\text{GeV}^2$								
$10^4 c$								15.4
$10^4$							0.07	1.2
$10^3 c$						0.07	0.3	1.0
$10^3$					0.1	0.4	0.5	1.1
$10^2 c$				0.2	0.7	0.9	0.8	1.1
$10^2$			0.2	0.9	1.4	1.3	1.0	1.1
$10^1 c$		0.3	1.1	1.7	2.0	1.7	1.1	1.1
10	0.5	1.9	3.3	4.4	4.7	3.8	2.6	2.1
$c/10^{-4}$	$c 10^{-4}$	$10^{-3}$	$c 10^{-3}$	$10^{-2}$	$c 10^{-2}$	$10^{-1}$	$c 10^{-1}$	1
$x_m \quad (c = \sqrt{10} \approx 3.16)$								

and the integration limits read

$$\frac{1 - x_m}{x_m} Q_l^2 \frac{Q_l^2}{y_l z s - Q_l^2} < Q_h^2 < y_l z s - \frac{1 - x_m}{x_m} Q_l^2$$

$$\text{Max} \left\{ \frac{W_{\min}^2 + Q_l^2}{y_l s}, \frac{Q_l^2}{y_l x_m s} \right\} < z < 1. \quad (17)$$

In tables 1 and 2 we present the size of the radiative corrections for (logarithmically distributed) bins ranging from  $10^{-4}$  up to 1 in  $x_m$  and  $3.2 \text{ GeV}^2$  up to  $3.2 \times 10^4 \text{ GeV}^2$  in  $Q_l^2$ . For example, the bin in the lower left corner corresponds to  $10^{-4} < x_m < 3.2 \times 10^{-4}$  and  $3.2 < Q_l^2 < 10 \text{ GeV}^2$ . The numbers are for a typical LEP kinematics, namely  $2 E_b = \sqrt{s} = 175 \text{ GeV}$ ,  $W_h > 2 \text{ GeV}$ , anti-tag angle  $\theta_{\max} = 30 \text{ mrad}$ , minimum tagging angle  $\theta_{\text{tag}} = 30 \text{ mrad}$ , minimum tagging energy  $E_{\text{tag}} = 0.5 E_b$ , and we have used the SaS 1D distribution functions of the photon [4]. While the corrections from the Compton process are small, the correction from initial-state radiation are sizeable and cannot be neglected.

As an example of the distortion of the Born (non-radiative) kinematics we show in Fig. 3 the distributions in  $Q_l^2$  and  $Q_h^2$  for the same kinematical situation: the scale entering the structure function ( $Q_h$ ) does differ substantially from the one ( $Q_l$ ) measured from the scattered electron. A Fortran program (“RADEG”) that computes the corresponding correction factors either for fixed  $x, y, Q^2$  or for user-defined bins in these variables, with integration inside the bin, is available from the authors.

## References

- [1] H. Spiesberger et al., in *Proc. of the Workshop on Physics at HERA* (Hamburg, Germany, 1991), eds. W. Buchmüller and G. Ingelman, p. 798.
- [2] M. Consoli and M. Greco, *Nucl. Phys. B* **186**, 519 (1981);  
W. Beenakker, F. Berends and W. van Neerven, in *Proc. of the Workshop on Radiative Corrections for  $e^+e^-$  Collisions* (Schloß Ringberg, Tegernsee, Germany, 1989), ed. J. Kühn, p. 3;  
J. Blümlein, *Z. Phys. C* **47**, 89 (1990);  
G. Montagna. O. Nicrosini and L. Trentadue, *Nucl. Phys. B* **357**, 390 (1991);  
J. Kripfganz, H. Möhring and H. Spiesberger, *Z. Phys. C* **49**, 501 (1991);  
A. Akhundov, D. Bardin, L. Kalinovskaya and T. Riemann, *Fortsch. Phys.* **44**, 373 (1996).
- [3] E. Laenen and G.A. Schuler, *Phys. Lett. B* **B374**, 217 (1996).
- [4] G.A. Schuler and T. Sjöstrand, *Z. Phys. C* **68**, 607 (1995).

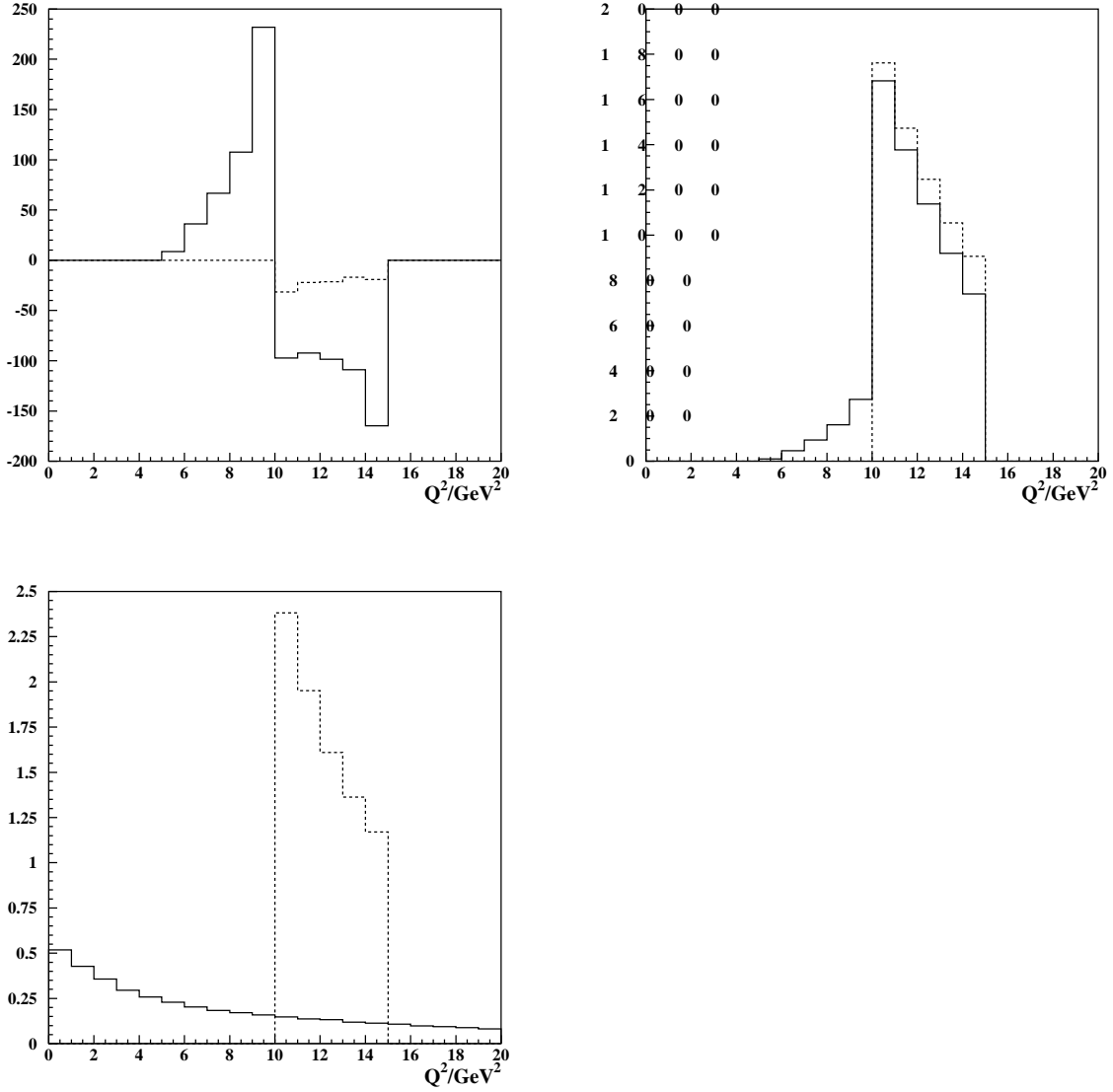


Figure 3:  $Q^2$  distributions of numbers of events (for an integrated luminosity of  $500 \text{ pb}^{-1}$ ) for initial-state radiation (upper left), the sum of Born and initial-state radiation (upper right) and Compton (lower left) events;  $Q_h^2$  distributions as solid lines,  $Q_l^2$  ones as dashed lines (parameters see text). The  $Q_l^2$  range was restricted to  $10 < Q_l^2 < 15 \text{ GeV}^2$ .



